9-1-2013

Changes in Hemodynamic Responses in Chronic Stroke Survivors Do Not Affect fMRI Signal Detection in a Block Experimental Design

Nutta-on Promjunyakul
Marquette University, nuttaon.promjunyakul@marquette.edu

Brian D. Schmit
Marquette University, brian.schmit@marquette.edu

Sheila Schindler-Ivens
Marquette University, sheila.schindler@marquette.edu

Accepted version. *Magnetic Resonance Imaging*, Vol. 31, No. 7 (September 2013): 1119-1128. DOI.

Changes in Hemodynamic Responses in Chronic Stroke Survivors Do Not Affect fMRI Signal Detection in a Block Experimental Design

Nutta-on Promjunyakul
Department of Physical Therapy
Department of Biomedical Engineering, Marquette University
Milwaukee, WI
Brian D. Schmit
Department of Biomedical Engineering, Marquette University
Department of Physical Medicine and Rehabilitation, Medical College of Wisconsin
Milwaukee, WI
Sheila Schindler-Ivens
Department of Physical Therapy
Department of Biomedical Engineering, Marquette University
Clinical and Translational Science Institute of Southeastern Wisconsin, Medical College of Wisconsin
Milwaukee, WI

Magnetic Resonance Imaging, Vol 31, No. 7 (September 2013): pg. 1119-1128. DOI.

Abstract

The use of canonical functions to model BOLD-fMRI data in people post-stroke may lead to inaccurate descriptions of task-related brain activity. The purpose of this study was to determine whether the spatiotemporal profile of hemodynamic responses (HDRs) obtained from stroke survivors during an event-related experiment could be used to develop individualized HDR functions that would enhance BOLD-fMRI signal detection in block experiments. Our long term goal was to use this information to develop individualized HDR functions for stroke survivors that could be used to analyze brain activity associated with locomotor-like movements. We also aimed to examine the reproducibility of HDRs obtained across two scan sessions in order to determine whether data from a single event-related session could be used to analyze block data obtained in subsequent sessions. Results indicate that the spatiotemporal profile of HDRs measured with BOLD-fMRI in stroke survivors was not the same as that observed in individuals without stroke. We observed small between-group differences in the rates of rise and decline of HDRs that were more apparent in individuals with cortical as compared to subcortical stroke. There were no differences in the peak or time to peak of HDRs in people with and without stroke. Of interest, differences in HDRs were not as substantial as expected from previous reports and were not large enough to necessitate the use of individualized HDR functions to obtain valid measures of movement-related brain activity. We conclude that all strokes do not affect the spatiotemporal characteristics of HDRs in such a way as to produce inaccurate representations of brain activity as measured by BOLD-fMRI. However, care should be taken to identify individuals whose BOLD-fMRI data may not provide an accurate representation of underlying brain activation when canonical models are used. Examination of HDRs need not be done for each scan session, as our data suggest that the characteristics of HDRs in stroke survivors are reproducible across days.

Keywords: Stroke, CVA, fMRI, Hemodynamic response function, Locomotion, Methods

1. Introduction

Blood oxygen level-dependent (BOLD) contrast functional magnetic resonance imaging (fMRI) has been used extensively to examine movement-related brain activity in people post-stroke. BOLD-fMRI is an indirect measure of brain activity that depends on coupling between neuronal activation and vascular responses triggered by changes in the ratio of oxygenated to deoxygenated hemoglobin [1,2]. Many studies use canonical functions to model task-related changes in brain activity measured with BOLD-fMRI. This approach assumes normal neurovascular coupling and normal hemodynamic responses

(HDRs) to local neuronal activity. However, these assumptions may not be correct for people post-stroke because stroke is a condition affecting cerebral blood vessels. Hence, the appropriate function for modeling HDRs after stroke may differ from the canonical functions used for the normal brain. The use of an inappropriate model may lead to inaccurate descriptions of task-related brain activity.

There is considerable evidence to suggest that the spatiotemporal characteristics of HDRs are abnormal after stroke and that these abnormalities result in inaccurate representations of brain activity as measured by BOLD-fMRI. Several investigators have reported delayed time to peak, decreased amplitude, and prolonged initial dip of HDRs measured from stroke survivors [3–7]. Others have shown that HDRs in this population were negative instead of positive for the entire duration of task performance [3–8] or attenuated in amplitude with task repetition [9]. When canonical functions developed for the normal brain were used to model stroke-related HDRs, little or no brain activation was detected with BOLD-fMRI despite normal task performance or unambiguous brain activation measured with magnetoencephalography (MEG) [3,10,11]. MEG measures magnetic fields produced by the brain, and it does not rely on vascular adaptations to neuronal activity. Hence, these data suggest that altered HDRs contribute to poor signal detection with BOLD-fMRI. Further support for this idea comes from observations wherein detection of brain activity with BOLD-fMRI was improved after canonical functions were modified to account for stroke-related changes in HDRs [5].

There are several possible approaches to enhancing the accuracy with which BOLD-fMRI can detect task-related brain activity after stroke. One option is to exclude stroke survivors with known compromise of cerebral blood flow, as abnormalities in HDRs are extensively documented in stroke survivors with cerebral artery occlusive disease [3,7,8,10] and in people without stroke who have complete or partial occlusion of cerebral vasculature [11–14]. A disadvantage of this approach is a smaller pool of stroke survivors from which to sample. Moreover, changes in the spatiotemporal profile of HDRs have also been observed in survivors of hemorrhagic and thromboembolic stroke [6] and strokes with no demonstrable cerebrovascular occlusion [4,5,7,9]. These data suggest that changes

in the vascular physiology that lead to stroke as well as those that result from stroke may contribute to abnormal HDRs (reviewed in [15]). Hence, the exclusion of stroke survivors with known compromise of cerebral blood flow may be inadequate for avoiding misinterpretation of BOLD-fMRI data.

Another possible solution is to analyze BOLD-fMRI data with techniques, such as deconvolution, that make no *a priori* assumptions about the spatiotemporal characteristics of HDRs. This approach is typically done in the context of event-related experimental designs that examine brief tasks with a clear start and end point. To address this issue for block designs, one might examine the spatiotemporal characteristics of HDRs during event-related experiments and to use this information to develop individualized functions to model the HDRs obtained during block designs. To our knowledge, this approach has not been attempted previously, and it is the focus of the present investigation. However, even this approach has practical limitations because it requires additional scanning time which could become problematic, particularly if an event-related protocol had to be added to every experimental session involving a block paradigm.

The purpose of this study was to determine whether the spatiotemporal characteristics of HDRs obtained from stroke survivors during an event-related paradigm could be used to develop individualized HDR functions that could be used to enhance BOLD-fMRI signal detection in block experiments. Our long term goal was to use this information to develop individualized HDR functions for stroke survivors that could be used to analyze brain activity associated with locomotor-like movements of the lower limbs. However, because locomotion is a continuous behavior, there is no event-related task from which to obtain the spatiotemporal profile of HDRs. Therefore, subjects performed foot tapping or knee flexion and extension, which are lower limb tasks that can be done in a continuous and discrete fashion. We obtained the spatiotemporal profile of HDRs from event-related lower limb movements and used this information to create individualized HDR functions for block data. Comparison was made between brain activations obtained when block data were processed with a normal canonical function and with individualized functions. We hypothesized that the spatiotemporal profile of HDRs measured from stroke survivors would be abnormal, resulting in poor detection of

movement-related brain activity with BOLD-fMRI when a normal canonical HDR function was used. We further predicted that detection of brain activity with BOLD-fMRI would be enhanced when individualized models were used. Finally, we examined the reproducibility of HDRs obtained across two scan sessions. We reasoned that, if the results were reproducible, then data from a single event-related session could be used to analyze block data obtained in subsequent sessions, which would eliminate the need to lengthen every scan session to include an event-related experiment.

2. Material and methods

2.1. Methods common to all experiments

Three experiments were performed. In this section, we present methods common to all experiments. Subsequent sections are devoted to methods unique to each experiment.

2.1.1. Subject preparation and set-up

All subjects gave written informed consent according to the Declaration of Helsinki and institutional guidelines at Marquette University and the Medical College of Wisconsin. Prior to participating, all subjects underwent MRI safety screening to ensure that they were not claustrophobic or pregnant and that they were free of implants or foreign bodies incompatible with MRI. Before fMRI scans, subjects participated in a familiarization session outside the MRI environment where we explained the experimental procedures and allowed them to practice the desired tasks until we were confident that they were capable of doing them correctly. During practice sessions we also explained the importance of remaining still during fMRI and encouraged subjects to keep their head and trunk stationary during all the movement tasks.

During fMRI scanning, subjects lay supine on the bed of a 3 TMRI scanner (General Electric Healthcare, Milwaukee, WI). The subject's head was placed in a single channel transmit/receive split head coil assembly (General Electric Healthcare model 2376114).To minimize movement, the head was enveloped by a beaded vacuum

pillow. Straps were also used to control head and trunk movement. Each subject wore MRI compatible earphones (model SRM 212, Stax Ltd, Japan) through which audio cues were delivered. An additional set of headphones was used to protect against scanner noise.

The legs were positioned over a foam bolster such that the hip and knees were flexed and the feet were approximately 15 cm above the surface of the scanner table. A circular plastic button (6.35 cm diameter) connected to a switch (Jelly Bean Twist Top Switch, AbleNet, Inc., Roseville, MN) was placed under the foot and was used to record lower limb movements. Each time the button was depressed a pulse was generated. These data were used to calculate movement rate and to ensure that subjects produced desired movements at appropriate times.

During each experiment, subjects' performance was visually monitored. We had access to real time information about head position. If the subject did not perform the task as instructed or if their head moved more than 2 mm, we checked the subject for comfort, repeated the instructions to remain still, and restarted the run. Efforts to minimize head movement during scans were successful, as head movement did not exceed 1.48 mm for control subjects and 0.35 mm for stroke subjects. A squeeze ball was placed near the subject's hands and could be used at any time to signal a problem. Participants were monitored for safety and comfort and were able to communicate via intercom with the scanner technician throughout the session.

2.1.2. Imaging parameters

Functional images (T2*-weighted) were acquired using gradient-echo echoplanar imaging (repetition time (TR): 2000 ms, echo time (TE): 25 ms, flip angle: 77°, NEX: 1, 36 contiguous slices in the sagittal plane, 64×64 matrix, 4 mm slice thickness, and field of view (FOV): 240 mm). The resolution of the images was 3.75×3.75×4 mm. Anatomical images (T1-weighted) were obtained approximately half way through the scan session using a spoiled GRASS pulse sequence (TR: 9.6 ms, TE: 39 ms, flip angle: 12°, 256×244 matrix, resolution: 1 mm^3, FOV: 240 mm, 148 slices in the sagittal plane, NEX: 1).

2.1.3. Data processing and statistics

Processing of fMRI signals was completed using Analysis of Functional NeuroImages (AFNI) software. All statistical analyses were completed in SPSS (SPSS Inc, Chicago, IL), and effects were considered significant at $P < 0.05$. Quantitative values are reported as mean ± 1 standard deviation (SD).

2.2. Experiment 1: Hemodynamic responses stroke versus control

2.2.1. Subjects

Thirteen individuals with chronic post-stroke hemiparesis (ST) (9 females, mean ± SD age 54.8 ± 12.8 years) and 9 age-matched control (C) subjects (6 females, mean ± SD age 54.3 ± 13.5 years) participated. ST participants had sustained a subcortical or cortical stroke at least 1.1 years prior to testing, and the mean ± SD time since stroke was 12.26 ± 13.1 years (See Table 1). There were 6 subjects with right and 6 subjects with left hemiparesis. One subject had stroke-related movement impairments on both sides. The mechanism of stroke was recorded from the medical record. Eight subjects had ischemic stroke. Of these eight, two had cerebrovascular occlusive disease at the time of stroke. Both had subsequently undergone carotid artery angioplasty. Four subjects had hemorrhagic stroke. In one subject, whose stroke occurred in infancy, we were unable to identify the cause. Individuals with stroke were divided into two groups according to lesion location: subcortical (STsc) and cortical (STc). The STsc group (n = 7) had brain injuries that involved the internal capsule, corona radiata, basal ganglia, or thalamus. Individuals in the STc group (n = 6) had injuries affecting one or more of the subcortical structures listed above, and they also had injuries involving a portion of the cerebral cortex outside of the leg area of the primary sensory and motor cortices (See Fig. 1). Control subjects had no signs or history of stroke or other neurological impairment.

Magnetic Resonance Imaging, Vol 31, No. 7 (September 2013): pg. 1119-1128. DOI.

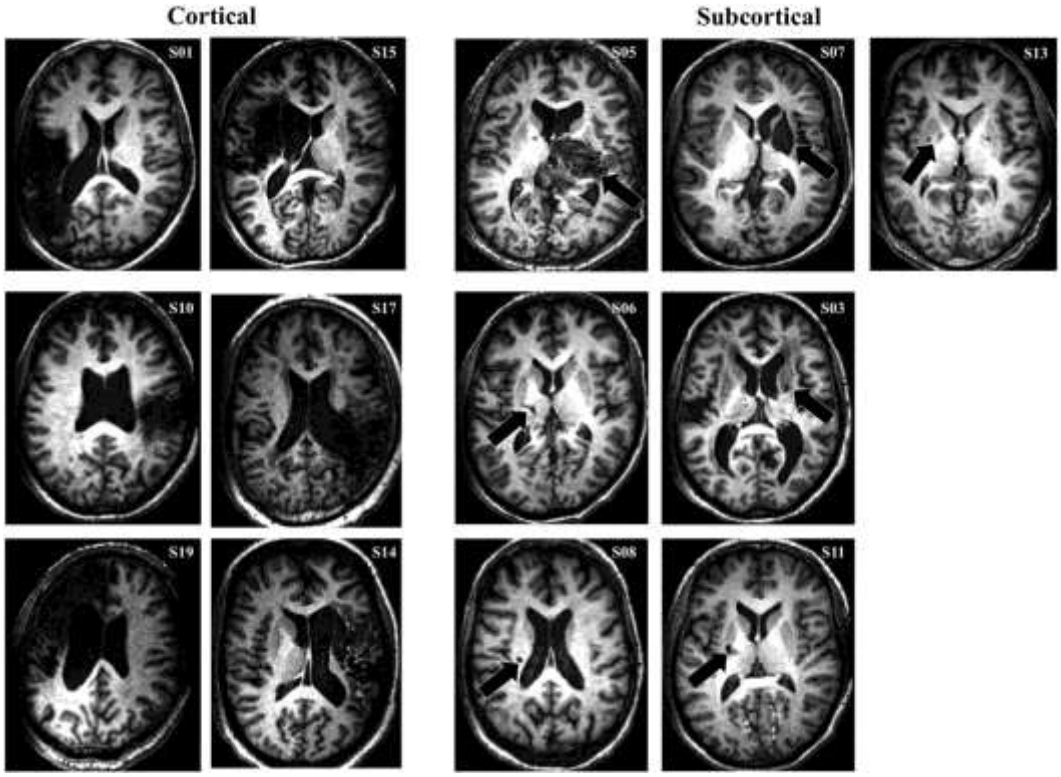

Fig. 1. T_1-weighted anatomical images displaying brain lesions of stroke subjects. Arrows are positioned to indicate lesion location. STc = subjects with cortical lesions, STsc = subjects with subcortical lesions, Left = left.

Table 1. Descriptive characteristics of stroke subjects.

Subject	Age (years)	Sex	Affected limb	Affected brain area	Lesion size (μL)	Time to scan	Mechanism of stroke
S01	60	F	R	Cortical	139120	20.4	I, E
S03	62	F	L	Subcor	157	8.4	I
S05	56	M	L	Subcor	51284	51.0	H, AVM
S06	64	F	R	Subcor	715	6.5	H
S07	20	F	L	Subcor	7623	19.0	U
S08	73	F	R	Subcor	156	1.1	I, E
S10	58	F	L	Cortical	40823	6.1	I, CVOD

Magnetic Resonance Imaging, Vol 31, No. 7 (September 2013): pg. 1119-1128. DOI.

Subject	Age (years)	Sex	Affected limb	Affected brain area	Lesion size (μL)	Time to scan (years)	Mechanism of stroke
S11	53	F	R	Subcor	600	17.4	I
S13	46	M	R > L	Subcor	1518	4.4	I
S14	52	F	L	Cortical	96263	4.3	H, ICAD
S15	48	M	R	Cortical	74433	8.1	H, ICAD
S17	65	F	L	Cortical	52811	6.2	I
S19	55	M	R	Cortical	136960	6.4	I, CVOD

F = female, M = male, R = right, L = left, Cortical = stroke affecting cerebral cortex, Subcortical = stroke affecting subcortical structures, I = ischemia, E = embolism, H = hemorrhage, AVM = arteriovenous malformation, U = unknown, CVOD = cerebrovascular occlusive disease, ICAD = internal carotid artery dissection.

2.2.2. Experimental protocol

Subjects were asked to tap one foot at a time on the button at a comfortable rate by dorsiflexing and plantarflexing the ankle. The left and right limbs were examined. A static tone indicated when to tap, and silence indicated rest. Knee flexion and extension was allowed in stroke participants (n = 7) who could not perform ankle movements.

An event-related design consisting of 3 runs was utilized. A single run included 20 moving events and 74 resting events, 2 s per event, presented in random order. Four additional acquisitions were made at the start of each run to account for unsteady state magnetization. Total scan time per run was 3 min and 16 s. This task was assumed to produce a brief burst of neuronal activity within the sensorimotor cortex (SMC). This design was created by AFNI sub-routine functions RSFgen and 3dDeconvolve with the -nodata option. RSFgen was used to generate the randomized event-related model for a given HDR duration and number of input stimuli. 3dDeconvolve with the -nodata option allowed us to evaluate the experimental design generated by RSFgen with respect to how well the HDR could be estimated without measured data.

2.2.3. Derivation of hemodynamic responses

Dicom files containing fMRI signals were converted into 3-dimensional images. Individual voxels were aligned to the same temporal origin within each TR. The first 4 TRs within each run were removed to eliminate non-steady state magnetization artifact. Multiple runs were concatenated and registered to the functional scan obtained closest in time to the anatomical scan. The measured time-series fMRI data were deconvolved with the input stimulus function to derive voxel-wise estimates of HDRs. This deconvolution was performed using the AFNI 3dDeconvolve function with maximum time lag of 15 TRs and 94 TRs for the fMRI response time series of a voxel (1 TR = 2 s). In the AFNI 3dDeconvolve function, the fMRI signal response is modeled as the sum of a baseline (e.g., a constant + linear trend) + the HDR convolved with the input stimulus + measurement noise as described by Ward [16]. Multiple linear regression with least-squares minimization was used to determine the HDR model parameters. Separate baseline estimates were made for each run. Estimated HDRs comprised 16 points, representing the response from 0 to 30 s after stimulus onset.

To identify voxels containing BOLD signals associated with the movement task, general linear modeling was performed using voxel-wise HDRs with head position as a variable of no interest. To identify significantly active voxels at a familywise error rate of $P < 0.05$, we used Monte Carlo simulation (AlphaSim) to set an appropriate cluster size for a given individual voxel P-value. Percent signal change was calculated as the change in amplitude of the BOLD signal from baseline. Significantly correlated voxels outside of the brain and negatively correlated voxels were ignored. Any voxels with percent signal change >10 were also ignored, as these large changes were likely due to edge effects.

For each subject, estimates of HDRs were obtained from the SMC contralateral to and ipsilateral to the moving limb. Because we tested the right and left limbs, a total of 4 HDRs were obtained. Each estimate was the average of the HDRs across all active voxels in the SMC, which included primary motor cortex (M1), primary sensory cortex (S1), and Brodmann's area 6. The anatomical boundaries for the SMC were defined from the T_1-weighted images as previously

described [17]. In the axial plane, the SMC extended anteriorly from the postcentral sulcus to cover approximately the posterior half of the superior frontal gyrus, and from the medial border of each hemisphere spanning laterally over the dorsolateral frontal lobe. In the sagittal plane, the SMC was bordered inferiorly by the cingulate sulcus, extending superiorly to the top of the hemisphere. Each subject's data were analyzed individually in its original coordinate system to avoid distortion arising from transformation to a standardized coordinate system.

2.2.4. Data analysis and statistics

Peak amplitude (PEAK), time to peak amplitude (TTP), and rate of change of amplitude (W) were measured from each estimated HDR for each subject. PEAK was defined as the maximum value of the HDR. TTP was defined as the length of time from the movement cue to PEAK. W was defined as the change in amplitude of the normalized HDR per TR, where normalization was accomplished by dividing the HDR by its amplitude at 6 s after stimulus onset. W was calculated for each of six different TRs beginning with the second TR after stimulus onset (W1: 2–4 s W2: 4–6 s, W3: 6–8 s, W4: 8–10 s, W5: 10–12 s, W6: 12–14 s). The rising portion of the HDR was represented in W1 and W2, and the declining portion was represented by W3-W6. See Fig. 2A.

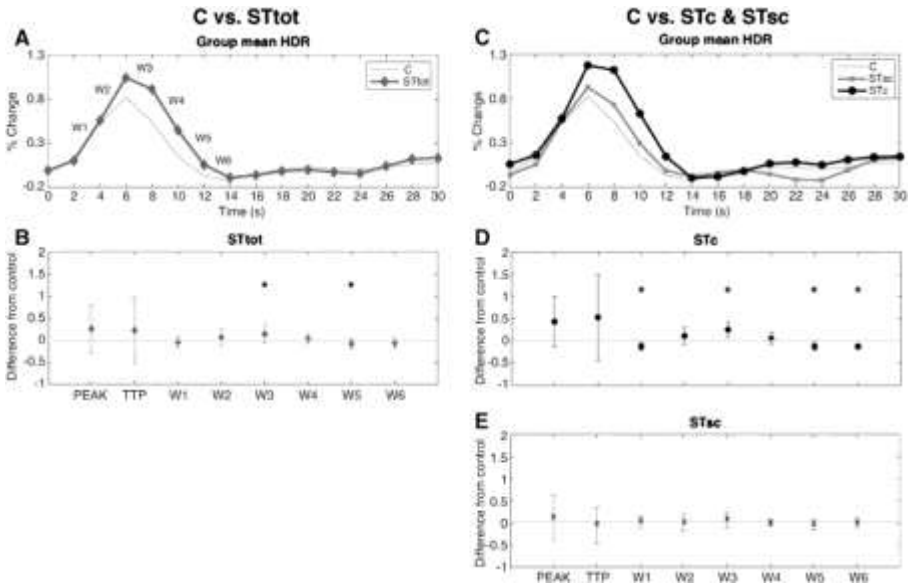

Fig. 2. Graphical representations comparing the spatiotemporal characteristics of hemomdynamic responses (HDRs) in individuals with and without stroke. A and C display the group mean time course of the HDRs observed in each group. B, D, and E represent mean (±SD) between-group differences for each dependent variable. PEAK = peak amplitude of the HDR, TTP = time to peak amplitude of the HDR, W = rate of change of amplitude of the HDR. Asterisks indicate significance at $P < 0.05$.

Multivariate analysis of variance (MANOVA) with repeated measures of the dependent variables was used to determine whether the estimates of the HDR in the C group were affected by moving limb (left versus right) or active hemisphere (ipsi- versus contralateral). No significant effect was identified ($P = 0.350$). Subsequently, we took the average across the four HDRs for each subject for each variable.

To test whether the HDRs recorded from the ST group were different from C, differences between each ST data point and the mean of the C group were calculated for each variable. These computations were completed for STsc and STc groups and for the entire sample of stroke survivors (STtot). MANOVA with repeated measures of the dependent variables was used to identify significant differences between each ST group and the C group and any interaction effects between the STc and STsc groups.

To understand the effect of active hemisphere, we split the data within each ST group into the HDRs associated with the undamaged and damaged hemispheres, regardless of moving limb. To understand the effect of the moving limb on the HDRs, we regrouped the data into the HDRs associated with the non-paretic and paretic limb movement, regardless of the active hemisphere. MANOVA with repeated measures of the dependent variables was used to identify differences between the undamaged and damaged hemispheres and differences between paretic and non-paretic limb movement.

We computed each subject's average movement rate across all trials and their average delay-to-stop moving. The latter was defined as the amount of time spent performing the movement task after the audio cue ended. Pearson correlation coefficients were calculated to examine the association between the characteristics of the HDRs and task performance.

Magnetic Resonance Imaging, Vol 31, No. 7 (September 2013): pg. 1119-1128. DOI.

2.3. Experiment 2: Canonical versus individualized hemodynamic response functions

2.3.1. Subjects

Six individuals with STc (4 females; age 56.3 ± 6 years) and 9 age-matched C subjects (6 females; age 54.3 ± 13.5 years), all of whom completed Experiment 1, participated. Only individuals with STc were examined here because the spatiotemporal profile of HDRs obtained from this subset of ST survivors was different from C.

2.3.2. Preparation, set-up, and experimental protocol

The experimental set-up and protocol were the same as in Experiment 1, except that we utilized a block design instead of an event-related design. The task comprised a single run of an ABABABABABABA pattern, where A represented a 16 s block of rest and B represented a 16 s block of movement. During the movement blocks, subjects were asked to tap their foot at a comfortable pace. Subjects who performed knee flexion and extension (n = 3) in Experiment 1 were allowed to perform the same movement here. A static tone indicated when to move; silence indicated rest. The left and right legs were examined separately.

2.3.3. Derivation of individualized hemodynamic response functions, data analysis, and statistics

To derive an individualized HDR function for each subject, the four different HDRs obtained for each subject in Experiment 1 were averaged, resulting in a single HDR for each subject. We then convolved each subject's average HDR with the block function used in this experiment. The result was an individualized HDR function for each subject.

To identify voxels containing movement-related brain activity, each subject's individualized HDR function was fit with the measured BOLD signal. Head position was used as a variable of no interest. As described previously [18], only the portion of the BOLD time-series after movement stopped was used. To compare detection power with

the normal canonical model, identical analysis with a canonical HDR function was performed.

The volume (VOL), intensity, and center of activation were used to assess detection power. For each subject, each variable was computed from bilateral SMC which was an area where we observed consistent activity across subjects. VOL was defined as the number of significantly active voxels in the SMC multiplied by voxel volume in microliters (μL). Intensity of activation was defined as the average percent signal change from baseline in the active portion of the SMC. Center of activation for activated clusters was reported as x, y, and z coordinates in original space.

MANOVA with repeated measures of VOL, intensity, and x, y, z coordinates of center of activation was used to compare canonical and individualized HDR functions with respect to signal detection power. This procedure was completed for left and right limb movement.

2.4. Experiment 3: Reproducibility

Eleven ST (7 females; age 53 ± 13.2 years, 5 STc, 6 STsc) and 9 age-matched C (6 females, age 54.3 ± 13.5 years) subjects who participated in Experiment 1 repeated the procedures from that experiment for the purpose of examining the reproducibility of the spatiotemporal characteristics of HDRs. The time elapsed between the first and the second session was 33.17 days (±66.85) and 9.33 days (±6.0) in the ST and C groups, respectively. The experimental set-up, protocol, data analysis and statistics were identical to Experiment 1. MANOVA with repeated measures of the dependent variables was used to identify between-day differences in PEAK, TTP, and W.

3. Results

3.1. Experiment 1: Hemodynamic responses stroke versus control

Contrary to expectations, there was no difference between the C and STtot groups with respect to the PEAK or TTP of the HDR. There was also no difference between these groups for rate of rise of the

HDR as represented by W1 and W2. The only differences in the HDR between the STtot and C groups occurred in the declining phase of the response where the initial portion of the decline (W3) occurred more gradually and the late portion of the decline (W5) happened more rapidly in the STtot as compared to the C group. See Fig. 2A and B for graphical representation and Table 2 for group means (±SD) and P-values.

Table 2. Group mean (±SD) values for peak amplitude (PEAK), time to peak amplitude (TTP), and rate of change of amplitude (W) of hemodynamic responses (HDRs) in all four groups examined.

			C	STtot	*P-value (C vs STtot)*	STc	*P-value (C vs STc)*	STsc	*P-value (C vs STsc)*
PEAK		Mean (±SD)	0.82 (±0.3)	1.09 (±0.5)		1.26 (±0.6)		0.94 (±0.5)	
		Diff from C		0.26 (±0.5)	0.105	0.43 (±0.6)	0.124	0.11 (±0.5)	0.567
TTP		Mean (±SD)	6.06 (±0.2)	6.26 (±0.8)		6.58 (±1.0)		6.00 (±0.4)	
		Diff from C		0.22 (±0.8)	0.315	0.53 (±1.0)	0.236	− 0.05 (±0.4)	0.757
Rate of change of amplitude	W1	Mean (±SD)	0.54 (±0.1)	0.48 (± 0.1)	0.292	0.40 (±0.1)	**0.020**	0.56 (±0.1)	0.619
		Diff from C		− 0.04 (±0.1)		− 0.13 (±0.1)		0.03 (±0.1)	
	W2	Mean (±SD)	0.34 (±0.1)	0.40 (±0.2)		0.45 (±0.2)		0.36 (±0.2)	
		Diff from C		0.06 (±0.2)	0.277	0.11 (±0.2)	0.257	0.02 (±0.2)	0.770
	W3	Mean (±SD)	− 0.34 (±0.1)	0.19 (±0.2)		− 0.09 (±0.2)		− 0.28 (±0.2)	
		Diff from C		0.14 (±0.2)	**0.018**	0.25 (±0.2)	**0.017**	0.06 (±0.2)	0.408
	W4	Mean (±SD)	− 0.45 (±0.1)	− 0.42 (±0.1)		− 0.40 (±0.1)		− 0.44 (±0.1)	

Magnetic Resonance Imaging, Vol 31, No. 7 (September 2013): pg. 1119-1128. DOI.

		C	STtot	*P-value (C vs STtot)*	STc	*P-value (C vs STc)*	STsc	*P-value (C vs STsc)*
	Diff from C		0.03 (±0.1)	0.371	0.05 (±0.1)	0.402	0.01 (±0.1)	0.824
W5	Mean (±SD)	− 0.25 (±0.1)	− 0.33 (±0.1)		− 0.38 (±0.1)		− 0.28 (±0.1)	
	Diff from C		− 0.08 (±0.1)	**0.045**	− 0.13 (±0.1)	**0.031**	− 0.03 (±0.1)	0.535
W6	Mean (±SD)	− 0.06 (±0.1)	− 0.11 (±0.1)		− 0.19 (±0.1)		− 0.05 (±0.1)	
	Diff from C		− 0.06 (±0.1)		− 0.13 (±0.1)	**0.003**	0.00 (±0.1)	0.898

C = control subjects, STtot = all stroke subjects, STc = subjects with cortical stroke, STsc = subjects with subcortical stroke. Significant between-group differences ($P < 0.05$) are represented in bold.

The spatiotemporal characteristics of HDRs were affected by stroke location. When we split the STtot group into STsc and STc, we found that the STc group had a slower rate of rise in W1, a slower rate of decline in W3, and a faster rate of decline in W5-W6, as compared to the C group. In contrast, we found that the STsc group was not significantly different from the C group with respect to any characteristics of the HDR. However, repeated MANOVA revealed no interaction between the STsc and STc groups. This observation suggests that that both ST groups were different from the C group in a similar fashion but that a cortical stroke may cause a more distinctive change in the HDR as compared to a subcortical stroke (See Fig. 2 C, D, and E and Table 2).

The spatiotemporal profile of the HDR was not affected by active hemisphere (undamaged versus damaged, $P = 0.208$)nor by the limb that was moving (non-paretic versus paretic, $P = 0.478$) (See Fig. 3).

Magnetic Resonance Imaging, Vol 31, No. 7 (September 2013): pg. 1119-1128. DOI.

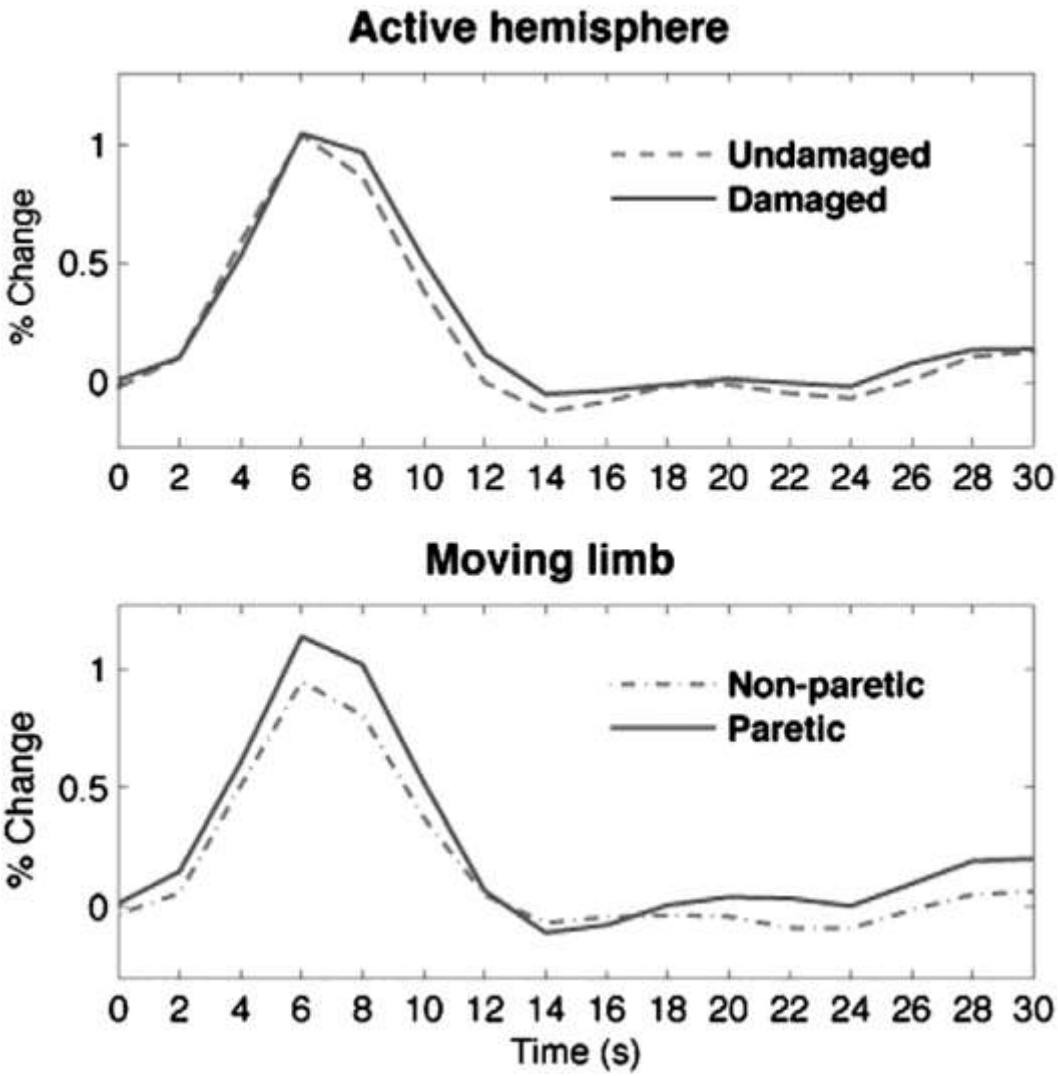

Fig. 3. Graphical representations comparing the spatiotemporal characteristics of hemomdynamic responses (HDRs) in individuals with stroke. Top figure compares the group mean time courses of the HDRs observed in the damaged and undamaged cortex. Bottom figure compares the group mean time courses of the HDRs observed during paretic and non-paretic limb movement.

It is possible that differences between the ST and C groups resulted from differences in task performance. Indeed, the STtot group moved at a slower rate than the C group (C = 1.92±0.6 Hz, STtot = 1.57± 0.4 Hz, P = 0.009), and within the STtot group, the paretic limb moved more slowly than the non-paretic limb (non-paretic = 1.69± 0.4 Hz, paretic = 1.42±0.4 Hz, P = 0.007). Delay-to-stop moving in the STtot group was not different from the C group (C = 0.66±0.3 s, STtot = 0.76±0.4 s, P = 0.405), but in the STtot group, the paretic leg

took longer to stop moving compared to the non-paretic leg (non-paretic =0.63±0.4 s, paretic = 0.91±0.3 s, P = 0.009). However, there was no significant correlation between movement rate and rate of rise in W1 (R = 0.208, P = 0.693). There was also no significant correlation between delay-to-stop and rate of decline in W3, W5, or W6 (R = 0.228, P = 0.664 for W3; R = −0.275, P = 0.597 for W5; R = 0.273,P = 0.600 for W6).

3.2. Experiment 2: Canonical versus individualized hemodynamic response functions

The HDR function used to fit the data (canonical versus individualized) had no effect on signal detection in the C or STc group. As shown in Fig. 4, there were no visually apparent differences between methods with respect to the size, shape, or location of brain activity observed in the SMC. Indeed, MANOVA results showed that there was no significant difference between methods with respect to VOL, intensity, or x, y, z coordinates of brain activity in the SMC. This observation was consistent for left and right limb movement in C subjects as well as paretic and non-paretic limb movement in the STc group (P = 0.128 for ST non-paretic, P = 0.277 for ST paretic, 0.623 for C left, 0.072 for C right) (See Fig. 5).

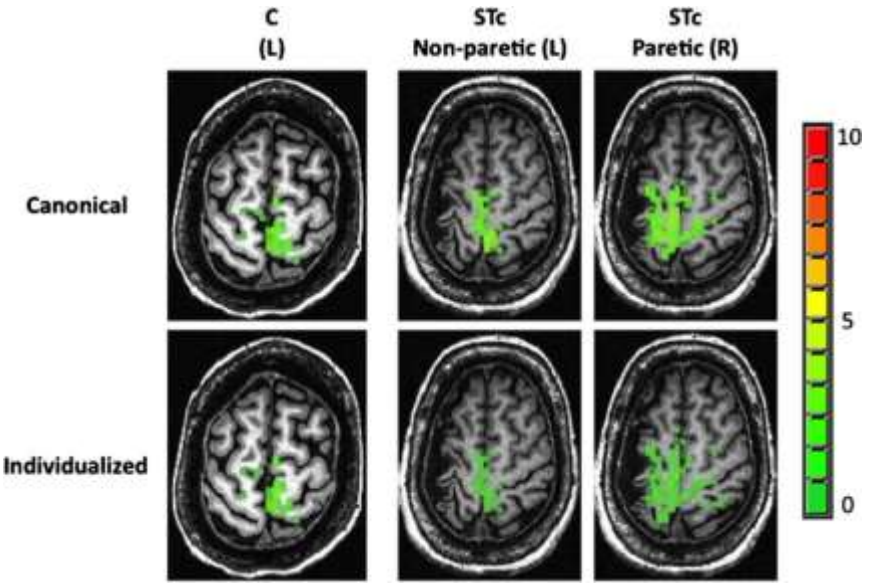

Fig. 4. Representative examples of brain activation maps derived from data processed with canonical and individualized models of HDRs. The color bar represents

percent signal change (0–10%). C (L) is a map from a single representative control subject tapping his left foot. STc Non-paretic (L) is a map from a representative subject with cortical stroke tapping with his non-paretic foot, which in this case is the left foot. STc Paretic (R) is a map from the same representative subject tapping with his paretic foot, which is his right foot.

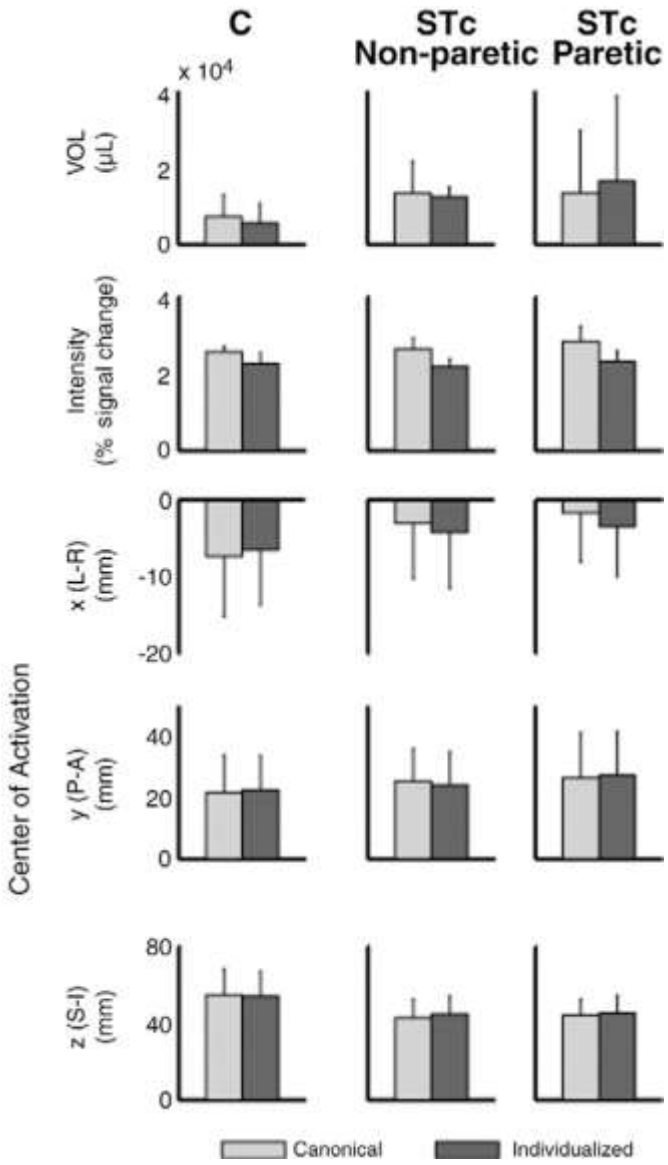

Fig. 5. Bar plots representing the volume (VOL), intensity, and center of activation (x, y, z) of brain activity obtained with canonical and individualized methods for processing BOLD-fMRI data. Values are group means (±SD). C = control subjects, STc = subjects with cortical lesions, Non-paretic = non-paretic limb moving, Paretic = paretic limb moving. L-R = left-right, P-A = posterior-anterior, S-I = superior-inferior.

Magnetic Resonance Imaging, Vol 31, No. 7 (September 2013): pg. 1119-1128. DOI.

3.3. Experiment 3: Reproducibility

As shown in Fig. 6, the spatiotemporal profiles of the HDRs recorded from ST and C subjects were repeatable across days. MANOVA with repeated measures revealed no between-day difference in the VOL, intensity, or x, y, z coordinates of brain activity during movement (P = 0.811 for C, P = 0.250 for STtot, P = 0.718 for STc, and P = 0.491 for STsc) (See Table 3 for mean (±SD) and P-values).

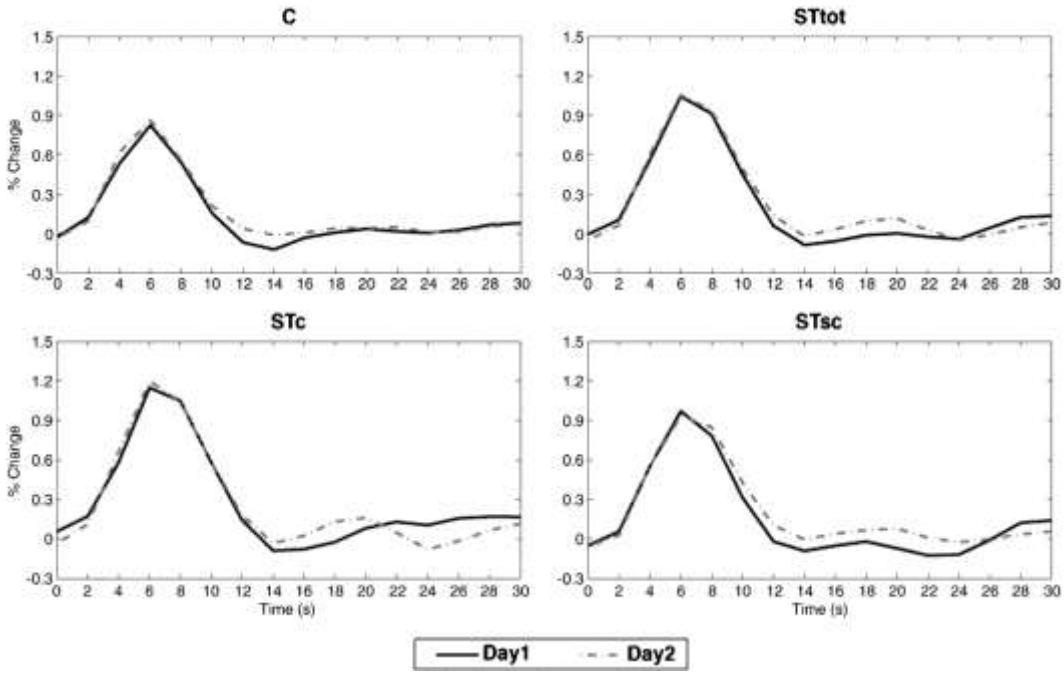

Fig. 6. Graphical representations comparing the group mean time courses of hemomdynamic responses (HDRs) obtained on two different days. C = control subjects, STtot = entire sample of stroke survivors, STc = subjects with cortical lesions, STsc = subjects with subcortical lesions.

Table 3. Group mean (±SD) values for peak amplitude (PEAK), time to peak amplitude (TTP), and rate of change of amplitude (W) of hemodynamic responses (HDRs) obtained on two different days.

		C		STtot		STc		STsc	
		Day1	**Day2**	**Day1**	**Day2**	**Day1**	**Day2**	**Day1**	**Day2**
PEAK		0.82 (±0.3)	0.91 (±0.5)	1.08 (±0.6)	1.10 (±0.5)	1.21 (±0.6)	1.23 (±0.6)	0.98 (±0.5)	0.99 (±0.4)
TTP		6.06 (±0.2)	5.91 (±0.8)	6.14 (±0.6)	6.32 (±0.6)	6.30 (±0.8)	6.30 (±0.3)	6.00 (±0.5)	6.33 (±0.8)
Rate of Change of Amplitude	W1	0.54 (±0.1)	0.63 (±0.2)	0.48 (±0.1)	0.55 (±0.1)	0.41 (±0.1)	0.51 (±0.2)	0.54 (±0.1)	0.59 (±0.1)
	W2	0.34 (±0.1)	0.25 (±0.2)	0.40 (±0.2)	0.41 (±0.2)	0.42 (±0.2)	0.41 (±0.1)	0.38 (±0.2)	0.40 (±0.3)
	W3	− 0.34 (±0.1)	− 0.30 (±0.2)	− 0.21 (±0.2)	− 0.14 (±0.2)	− 0.14 (±0.1)	− 0.15 (±0.1)	− 0.27 (±0.2)	− 0.13 (±0.2)
	W4	− 0.45 (±0.1)	− 0.40 (±0.1)	− 0.43 (±0.1)	− 0.40 (±0.1)	− 0.38 (±0.2)	− 0.35 (±0.1)	− 0.46 (±0.1)	− 0.45 (±0.1)
	W5	− 0.25 (±0.1)	− 0.21 (±0.1)	− 0.31 (±0.1)	− 0.31 (±0.1)	− 0.35 (±0.1)	− 0.31 (±0.1)	− 0.29 (±0.1)	− 0.32 (±0.1)
	W6	− 0.05 (±0.1)	− 0.08 (±0.1)	− 0.11 (±0.1)	− 0.13 (±0.1)	− 0.18 (±0.1)	− 0.17 (±0.1)	− 0.05 (±0.1)	− 0.10 (±0.1)
P-value		0.811		0.250		0.718		0.491	

C = control subjects, STtot = all stroke subjects, STc = subjects with cortical stroke, STsc = subjects with subcortical stroke. P-values represent within-group comparisons for Day 1 versus Day 2.

4. Discussion

Consistent with our hypothesis, this study showed that the spatiotemporal profile of HDRs measured with BOLD-fMRI in stroke survivors was not the same as that observed in individuals without stroke. However, these differences were not as substantial as expected from previous reports and were not large enough to necessitate the

use of individualized HDR functions to obtain valid measures of movement-related brain activity. Specifically, we observed small between-group differences in the rates of rise and decline of HDRs that were more apparent in individuals with cortical as compared to subcortical stroke. There were no differences in the PEAK or TTP of HDRs in people with and without stroke. We conclude that all strokes do not affect the spatiotemporal characteristics of HDRs in such a way as to produce inaccurate representations of brain activity as measured by BOLD-fMRI. Nevertheless, care should be taken to identify individuals whose BOLD-fMRI data may not provide an accurate representation of underlying brain activation when canonical models are used for data processing. One approach for identifying these individuals is to use an event-related paradigm and deconvolution algorithms to examine the spatiotemporal characteristics of HDRs, as we did here. Examination of HDRs need not be done for each scan session, as our data suggest that the characteristics of HDRs in stroke survivors are reproducible across days.

4.1. Similarities in HDRs in people with and without stroke

The most striking finding of this study was the absence of major changes in the spatiotemporal profile of HDRs in people post-stroke that interfered with detection of task-related brain activity as measured with BOLD-fMRI. This observation is different from other studies reporting poor detection of brain activity with BOLD-fMRI when data were processed with canonical HDR functions developed for the normal brain [9–11,14]. Impaired detection of task-related brain activity with BOLD-fMRI in people post-stroke has been attributed to abnormal spatiotemporal characteristics of HDRs [10,11,14]. Indeed, previous studies have reported markedly abnormal HDRs in stroke survivors that were characterized by delayed TTP, decreased PEAK, prolonged initial dip, and completely negative responses [3–9]. These abnormalities have been attributed to changes in neurovascular coupling which is the process by which neural activity triggers blood flow changes that decrease the ratio of deoxygenated to oxygenated hemoglobin in local vasculature. These processes result in an increase in the BOLD-fMRI signal. Hence, our observations suggest that the stroke survivors examined here had more normal neurovascular

coupling than many stroke survivors examined previously and that stroke is not always associated with impaired neurovascular coupling that leads to poor detection of brain activity with BOLD-fMRI.

Abnormal neurovascular coupling post-stroke has been attributed to poor cerebrovascular autoregulation caused by cerebrovascular occlusive disease. Unlike the present study, many previous studies have examined HDRs in individuals with cerebrovascular occlusive disease characterized by high grade stenosis or occlusion of the internal carotid or middle cerebral arteries [3,5,7,10–12,14]. In these studies, impaired autoregulation of cerebral vasculature can explain the observed changes in the spatiotemporal profile of HDRs and subsequent poor detection of brain activity with BOLD-fMRI. Autoregulation is the process whereby cerebral blood vessels alter blood flow by altering vessel diameter. In the presence of cerebrovascular occlusive disease, the brain is in a state of chronic hypoperfusion resulting in compensatory vasodilation. Autoregulation to task-related neural activity may be diminished because cerebral blood vessels are already maximally dilated. Moreover, even if cerebral blood vessels are not maximally dilated, their response to neural activity may be sluggish because of structural changes affecting the elasticity of vessel walls such as thickening of the basement membrane, thinning of the endothelium, or plaque formation [15]. Further support for impaired autoregulation as an explanation for abnormal HDRs comes from studies demonstrating that stroke survivors with abnormal vasomotor reactivity were more likely that those with normal vasomotor reactivity to have abnormal HDRs [10]. Similar results have been observed in individuals with cerebrovascular occlusive disease who have not experienced a stroke [12–14], which further suggests that cerebrovascular occlusive disease is an important contributor to abnormal HDRs.

Unlike many existing publications on HDRs post-stroke, the subjects in the present study displayed scant evidence of cerebrovascular occlusive disease. This observation likely explains differences between our results and those reported previously. As shown in Table 1, four subjects had hemorrhagic strokes that were caused by arterial venous malformation or internal carotid artery dissection. Eight subjects experienced ischemic strokes. Of those eight, two had significant cerebrovascular stenosis at the time of

stroke. Both of these subjects had subsequently undergone carotid artery angioplasty to improve cerebral perfusion. In the remaining subjects with ischemic stroke, cerebrovascular stenosis ranged from zero to <50% occlusion. Significant occlusion is typically defined as ≥70% occlusion. We were unable to identify the cause of stroke in 1 subject, but it occurred in infancy, and the subject was only 21 years of age when we studied her. Thus, it seems unlikely that she had cerebrovascular occlusive disease. Hence, we conclude that the absence of substantial changes in HDRs that affect signal detection in the subjects examined here can be explained by the absence of cerebrovascular occlusive disease and normal autoregulation.

4.2. Differences in HDRs in people with and without stroke

Having ruled out cerebrovascular occlusive disease as an important contributor to the spatiotemporal characteristics of the HDRs observed here, tissue damage caused by stroke is a plausible explanation for between-group differences. Bonakdapur et al. [6] reported altered HDRs post-stroke in the absence of significant cerebrovascular stenosis. This group reported that abnormal HDRs in stroke survivors were observed predominantly in damaged regions of the brain. They suggested that lesion-related damage to the vascular bed supplying the cortex may have caused these changes. Of interest, there was one subject (also free of cerebrovascular occlusive disease) who had abnormal HDRs on the damaged and intact sides of the brain. This individual had the most extensive stroke-related brain damage of all the subjects examined, and he had a closed head injury prior to a stroke. In light of this observation, Bonakdapur's group suggested that the extensiveness of his brain injury may have resulted in extensive and diffuse damage to the vascular bed. In turn, this damage may have led to abnormal neurovascular coupling and abnormal HDRs across the entire brain.

Lesion-induced changes in the vascular bed may also explain why the HDRs seen here differed with lesion location (cortical versus subcortical). If brain damage disrupts the vascular bed and changes neurovascular coupling, then one can reason that the more extensive the tissue damage, the more abnormal the HDR. The STc subjects

tested in the present study had more extensive brain damage than subjects in the STsc group. The STc group also showed more distinctive changes in the HDR as compared to the STsc group. Consistent with the observations of Bonakdapur et al., vascular bed damage may account for these changes. In subcortical stroke, vascular changes in the brain may be distant from the gray matter where the BOLD-fMRI signal is recorded. Consequently, these changes may have only a minimal effect on the signal. This conclusion is further supported by literature suggesting that altered HDRs are not observed in diaschesis [19], which is a condition characterized by loss of function in a portion of the brain that is distant from the lesion.

Behavioral explanations for between-group differences are unlikely. Indeed, the ST group moved more slowly than the C group. However, slow movement would likely be associated with a lower than normal PEAK because the amplitude of HDRs increases with movement rate [20,21]. Here, we saw larger values for PEAK in the ST group as compared to C. It is also unlikely that behavior explains the slower rate of decline in the ST group as compared to C, as stroke survivors did not have a longer delay-to-stop moving than C subjects.

4.3. Canonical versus individualized models

Contrary to our prediction, detection of brain activity with BOLD-fMRI was not enhanced when individualized models of HDRs were used in place of normal canonical functions. This result differs from previous observations [6,7,9] but is not surprising in light of knowledge that the spatiotemporal profile of HDRs was not dramatically different in the stroke and control subjects examined here. These data suggest that the use of a normal canonical model is appropriate for processing movement-related brain activity in people with stroke, provided that changes in the characteristics of HDRs are within the range of values observed here. This conclusion is not in conflict with prior reports of enhanced sensitivity of BOLD-fMRI with individualized models where substantial changes in the characteristics of HDRs were observed. Indeed, there is likely a threshold beyond which canonical functions do not accurately model HDRs in people post-stroke. Unfortunately, we cannot determine when individualized models become necessary because there was a limited range of variability in the characteristics

of the HDRs observed here, and no subject's functional brain activity was substantially changed by the individualized model. Future studies should make an effort to identify individuals with a variety of altered HDRs to determine under what circumstances individualized models are needed. Meanwhile, the prudent investigator should use caution in applying canonical functions to BOLD-fMRI data recorded from stroke survivors with cerebrovascular occlusive disease, as the literature has repeatedly shown abnormal HDRs in this population. Moreover, even in the absence of significant cerebrovascular occlusive disease, investigators should examine the spatiotemporal profile of HDRs recorded from stroke survivors to confirm that changes are qualitatively and quantitatively similar to those observed here before applying a canonical function.

Also because HDRs were not dramatically different between stroke and control subjects, this study unable to assess the effectiveness of individualized models for enhancing BOLD-fMRI signal detection in stroke survivors with abnormal HDRs. We consider that the similarity of results obtained from the canonical and individualized approaches was due to the lack of substantial changes in the HDRs recorded from stroke survivors. We still do not know whether our approach, whereby the characteristics of HDRs derived from an event-related task were used to create a function for modeling block data, enhances BOLD-fMRI signal detection. Additional studies that identify stroke survivors with abnormal HDRs are needed to examine the usefulness of this approach.

4.4. Reproducibility

Our data suggest that examination of the spatiotemporal profile of HDRs need not be done for each scan session, as our data demonstrate that the characteristics of HDRs in stroke survivors are reproducible across days. One other study has demonstrated reproducibility of HDRs across days in control subjects [22], but to our knowledge, this is the first of such demonstrations in stroke survivors. This observation has practical utility because it suggests that an event-related protocol to examine the spatiotemporal characteristics of HDRs need not be added each time an fMRI study is completed. Instead, the results of a single experiment can be applied for subsequent

experiments provided that the two sessions are within approximately one month of each other and stroke survivors are in the chronic stage of recovery. However, the reproducibility of the HDRs across days in acute and sub-acute stroke survivors may not be as robust, because vascular events associated with acute stroke and the early stages of recovery cause transient changes in neurovascular coupling [15].

5. Conclusion

This paper demonstrates that, in the context of a block design fMRI experiment, canonical models developed for the normal brain can be as effective as individualized models for accurate representation of task-related brain activity in stroke survivors. This finding can be attributed to the absence of dramatic abnormalities in the spatiotemporal profiles of the HDRs in stroke survivors without cerebrovascular occlusive disease. However, before applying canonical functions to stroke data, one should verify that HDRs in the sample of interest are no more abnormal that those seen here. Examination of HDRs need not be performed on the same day as the block design, as the spatiotemporal profile of HDRs is reproducible across days.

Acknowledgments

We would like to thank Matthew Verber and Naveen Bansal for their contributions to this work. This study was supported by a grant from the National Center for Medical and Rehabilitation Research at the National Institute of Child Health and Human Development awarded to SS-I. The funding source had no role in the study design; in the collection, analysis, or interpretations of data; in the writing of the report; or in the decision to submit the article for publication.

Glossary

AFNI	analysis of function images software
BOLD	blood oxygen level-dependent
C	control
fMRI	functional magnetic resonance imaging

HDR	hemodynamic responses
L	left
M1	primary motor cortex
MANOVA	multivariate analysis of variance
MEG	magnetoencephalography
PEAK	peak amplitude
R	right
S1	primary sensory cortex
SD	standard deviation
SMC	sensorimotor cortex
ST	stroke
STc	stroke cortical
STsc	stroke subcortical
STtot	entire sample of stroke survivors
TTP	time to peak
VOL	volume
W	rate of change of amplitude

References

1. Kwong KK, Belliveau JW, Chesler DA, Goldberg IE, Weisskoff RM, Poncelet BP, et al. Dynamic magnetic resonance imaging of human brain activity during primary sensory stimulation. Proc Natl Acad Sci U S A. 1992;89(12):5675–5679.
2. Ogawa S, Tank DW, Menon R, Ellermann JM, Kim SG, Merkle H, et al. Intrinsic signal changes accompanying sensory stimulation: functional brain mapping with magnetic resonance imaging. Proc Natl Acad Sci U S A. 1992;89(13):5951–5955.
3. Roc AC, Wang J, Ances BM, Liebeskind DS, Kasner SE, Detre JA. Altered hemodynamics and regional cerebral blood flow in patients with hemodynamically significant stenoses. Stroke. 2006;37(2):382–387.
4. Pineiro R, Pendlebury S, Johansen-Berg H, Matthews PM. Altered hemodynamic responses in patients after subcortical stroke measured by functional MRI. Stroke. 2002;33(1):103–109.
5. Altamura C, Reinhard M, Vry MS, Kaller CP, Hamzei F, Vernieri F, et al. The longitudinal changes of BOLD response and cerebral hemodynamics from acute to subacute stroke. A fMRI and TCD study. BMC Neurosci. 2009;10:151.

6. Bonakdarpour B, Parrish TB, Thompson CK. Hemodynamic response function in patients with stroke-induced aphasia: Implications for fMRI data analysis. Neuroimage. 2007;36(2):322–331.
7. Newton J, Sunderland A, Butterworth SE, Peters AM, Peck KK, Gowland PA. A pilot study of event-related functional magnetic resonance imaging of monitored wrist movements in patients with partial recovery. Stroke. 2002;33(12):2881–2887.
8. Fridriksson J, Rorden C, Morgan PS, Morrow KL, Baylis GC. Measuring the hemodynamic response in chronic hypoperfusion. Neurocase. 2006;12(3):146–150.
9. Mazzetto-Betti KC, Leoni RF, Pontes-Neto OM, Santos AC, Leite JP, Silva AC, et al. The stability of the blood oxygenation level-dependent functional MRI response to motor tasks is altered in patients with chronic ischemic stroke. Stroke. 2010;41(9):1921–1926.
10. Rossini PM, Altamura C, Ferretti A, Vernieri F, Zappasodi F, Caulo M, et al. Does cerebrovascular disease affect the coupling between neuronal activity and local haemodynamics? Brain. 2004;127((Pt 1)):99–110.
11. Murata Y, Sakatani K, Hoshino T, Fujiwara N, Kano T, Nakamura S, et al. Effects of cerebral ischemia on evoked cerebral blood oxygenation responses and BOLD contrast functional MRI in stroke patients. Stroke. 2006;37(10):2514–2520.
12. Carusone LM, Srinivasan J, Gitelman DR, Mesulam MM, Parrish TB. Hemodynamic response changes in cerebrovascular disease: implications for functional MR imaging. AJNR Am J Neuroradiol. 2002;23(7):1222–1228.
13. Rother J, Knab R, Hamzei F, Fiehler J, Reichenbach JR, Buchel C, et al. Negative dip in BOLD fMRI is caused by blood flow-oxygen consumption uncoupling in humans. Neuroimage. 2002;15(1):98–102.
14. Hamzei F, Knab R, Weiller C, Rother J. The influence of extra- and intracranial artery disease on the BOLD signal in FMRI. Neuroimage. 2003;20(2):1393–1399.
15. Marshall RS. The functional relevance of cerebral hemodynamics: why blood flow matters to the injured and recovering brain. Curr Opin Neurol. 2004;17(6):705–709.
16. Ward B. Deconvolution analysis of fMRI time series data.AFNI 3dDeconvolve documentation. Medical College of Wisconsin; 2006. Available at: http://afni.nimh.nih.gov/pub/dist/doc/manual/Deconvolvem.pdf.
17. Wexler BE, Fulbright RK, Lacadie CM, Skudlarski P, Kelz MB, Constable RT, et al. An fMRI study of the human cortical motor system response to increasing functional demands. Magn Reson Imaging. 1997;15(4):385–396.

18. Mehta J, Verber M, Wieser J, Schmidt B, Schindler-Ivens SM. A novel technique for examining human brain activity associated with pedaling using fMRI. J Neurosci Methods. 2009
19. Fair DA, Snyder AZ, Connor LT, Nardos B, Corbetta M. Task-evoked BOLD responses are normal in areas of diaschisis after stroke. Neurorehabil Neural Repair. 2009;23(1):52–57.
20. Lutz K, Koeneke S, Wustenberg T, Jancke L. Asymmetry of cortical activation during maximum and convenient tapping speed. Neurosci Lett. 2005;373(1):61–66.
21. Rao SM, Bandettini PA, Binder JR, Bobholz JA, Hammeke TA, Stein EA, et al. Relationship between finger movement rate and functional magnetic resonance signal change in human primary motor cortex. J Cereb Blood Flow Metab. 1996;16(6):1250–1254.
22. Aguirre GK, Zarahn E, D'esposito M. The variability of human, BOLD hemodynamic responses. Neuroimage. 1998;8(4):360–369.